



# Optical coherence tomography angiography characteristics of choroidal melanoma

Nan Zhou<sup>1</sup> · Xiaolin Xu<sup>1</sup> · Wenbin Wei <sup>1</sup>

Received: 3 June 2020 / Revised: 24 August 2020 / Accepted: 21 October 2020 / Published online: 9 November 2020  
© The Author(s), under exclusive licence to The Royal College of Ophthalmologists 2020

## Abstract

**Purpose** The purpose of this study is to evaluate tumour vasculature with optical coherence tomography angiography (OCTA) in malignant choroidal melanoma (CM).

**Materials and methods** Patients with unilateral CM were included in this cross-sectional observational clinical study. Applying OCTA systems operating at 840-nm wavelengths, eyes with CM were imaged. The primary main outcome measures were OCTA images, qualitative evaluation of macular and tumour vasculature, quantitative vascular density (VD), perfusion density (PD) and the foveal avascular zone disruption.

**Results** The study included 11 patients with unilateral CM and contralateral unaffected eyes as the control group. Eyes of 11 patients with CM and contralateral unaffected eyes were imaged before brachytherapy and 5 patients were imaged post brachytherapy. CM is demonstrated dense, tortuous blood vessels, uneven thickness and relatively disorganised intratumoural vasculature. In 11 eyes with CM, the VD and PD in the macular area were significantly lower within affected eyes ( $131.333 \pm 27.807\%$ ,  $3.152 \pm 0.714\%$ ,  $p < 0.0001$ ) than in contralateral eyes ( $154.208 \pm 5.599\%$ ,  $3.662 \pm 0.127\%$ ,  $p < 0.0001$ ). The VD and PD in the tumour area ( $67.990 \pm 34.899\%$ ,  $1.617 \pm 0.847\%$ ,  $p < 0.0001$ ) were significantly lower when compared to the macular area of affected eyes ( $131.333 \pm 27.807\%$ ,  $3.152 \pm 0.714\%$ ,  $p < 0.0001$ ) and the macular area of contralateral eyes ( $154.208 \pm 5.599\%$ ,  $3.662 \pm 0.127\%$ ,  $p < 0.0001$ ). After radiation treatment, the VD and PD in five CM eyes ( $116.526 \pm 7.598\%$ ,  $2.438 \pm 0.358\%$ ,  $p < 0.05$ ) were significantly lower than before treatment ( $141.544 \pm 14.645\%$ ,  $3.327 \pm 0.354\%$ ,  $p < 0.05$ ). Tumour regression after radiation therapy for melanomas was associated with decreased vessel density.

**Conclusions** OCTA can provide a dye-free, non-invasive, reliable method to monitor a variety of tumours, including CM for growth and vascularity. Upon OCTA, this could be helpful in evaluating the variety of tumour blood vessels before and after brachytherapy to judge the curative effect and whether the tumour recurred. Detection of the characteristic vascular features of CM by OCTA could make OCTA an assuring diagnostic modality to differentiate malignant lesions.

## Introduction

Optical coherence tomography angiography (OCTA) is a relatively new, non-invasive and non-contact microvascular imaging technique. It can image angiography by detecting changes in the optical coherence tomography (OCT) signal when flowing blood cells pass through the vascular cavity.

The method does not need to inject contrast agent, which makes it safer and more convenient than conventional fundus angiography techniques, such as indocyanine green angiography (ICGA) and fluorescein angiography (FA). OCTA was originally applied to evaluate retinal vascular diseases or choroidal neovascularization [1, 2]. Analyzation and evaluation of tumour vasculature in humans by OCTA is a newly developing field [3, 4]. We applied an OCTA system working at 840-nm wavelength, which can provide the sufficient penetration of tumour tissues and investigate OCTA in choroidal melanoma (CM).

CM is the most common primary intraocular malignancy in adults, with an incidence of ~5–6 cases per million population [5–7]. Eye-sparing treatment with brachytherapy is the main conservative treatment of CM and achieves local

✉ Wenbin Wei  
weiwenbintr@163.com

<sup>1</sup> Beijing Tongren Eye Center, Beijing Key Laboratory of Intraocular Tumor Diagnosis and Treatment, and Beijing Ophthalmology and Visual Science Key Lab, Beijing Tongren Hospital, Capital Medical University, Beijing, China

**Table 1** Baseline tumour features of the study population.

Case	The largest basal diameter, mm	Tumour thickness, mm	Tumour location	Distance to the macula, DD	Ultrasound reflectivity	Associated findings
1	7.5	3.50	MP	2	DSHFM	SWR, ERD
2	5.8	4.80	MP	1–2	DSHFM	ERD
3	6.5	5.37	MP	2	DSHFM	SWR, ERD
4	10.0	6.46	MP	2	DSHFM	SWR, ERD
5	9.6	3.21	PM	2–3	DSHFM	SWR, ERD
6	5.6	3.46	PM	2–3	DSHFM	ERD
7	6.0	1.31	PM	1–2	DSHFM	SWR
8	4.9	3.22	M	/	DSHFM	SWR, ERD
9	5.5	2.10	PM	1	DSHFM	SWR
10	6.1	3.53	PM	0–1	DSHFM	SWR
11	3.9	2.81	PM	0–1	DSHFM	SWR

*DD* disk diameter, *MP* midperipheral, *PM* perimacular, *M* macula, *SWR* surface-wrinkling retinopathy, *ERD* exudative retinal detachment, *DSHFM* dome-shaped hyperreflective mass.

control in around 94–96% of the patients at 5-year follow-up [8–11]. Diagnosis is based on indirect ophthalmoscope features and ancillary imaging tests, and follow-up needs the help of ultrasonography, OCT and FA/ICGA. One of the important clinical signs that may be indicative of a more aggressive neoplasm with metastatic potential is increased blood vessels. OCTA is a non-invasive imaging modality that can construct a map of blood flow in various layers using specialised algorithms. OCTA further provides an opportunity to generate quantitative indicators to describe the status of the tumour vasculature.

In this study, we used the OCTA to characterise CM and compare vascular morphology, vascular density (VD, defined as the total length of perfused vasculature per unit area in a region of measurement) and perfusion density (PD, defined as the total area of perfused vasculature per unit area in a region of measurement) in tumours, the macular area with contralateral eyes, to evaluate vascular changes in tumour blood vessels related to tumorigenesis. We also demonstrated OCTA imaging of CMs treated with radioactive I-125 plaque brachytherapy to evaluate changes in vasculature associated with tumour control after radiotherapy.

## Participants and methods

Participants of the cross-sectional observational study were recruited at Beijing Tongren Eye Center, Beijing Tongren Hospital (Capital Medical University, Beijing Key Laboratory of Intraocular Tumor Diagnosis and Treatment and Beijing Ophthalmology & Visual Science Key Laboratory of Beijing, China) from January 2018 to April 2019. This study followed the tenets of the Declaration of Helsinki and was in accordance with the Health Insurance Portability and Accountability Act of 1996. Clinical trial

registration was not required due to the observational nature of the study. All subjects were at least 18 years old. Written informed consent was obtained from all subjects.

## Clinical examination

All patients with CM underwent standard clinical evaluation, including best-corrected visual acuity measurement with Snellen charts, slit-lamp examination, dilated fundus examination and imaging with fundus colour photography, colour Doppler ultrasonography (CDI), ICGA and FA and OCTA images. Clinical diagnosis of CM was based on the presence of the features of fundoscopic examination, the classical clinical characteristics of colour Doppler imaging (CDI) examination, magnetic resonance imaging findings, fluorescein fundus angiography and ICGA findings. The clinical evaluation and imaging reviewing were conducted by an ophthalmic oncologist (WW) with rich experience in the clinical diagnosis of CM.

Exclusion criteria were clinically relevant opacities of the optic media, uncooperative, previously treated or low-quality images obtained with OCTA due to the thickness of tumours.

The mean tumour thickness was measured with standardised ultrasonography before and after plaque brachytherapy.

Baseline tumour features include the largest basal diameter, tumour thickness, tumour location, distance to the macula, ultrasound reflectivity and the associated findings (Table 1). Under careful imaging examination, 96% of the subjects obtained interpretable OCTA images.

## OCTA

Each eye of each CM patient was evaluated with a commercially available AngioPlex instrument (Cirrus 5000 HD-

**Table 2** Panel a: demographic characteristics and quantitative analysis of vascular density between CM and macular areas of affected eyes and contralateral/control eyes; panel b: quantitative analysis of perfusion density between CM and macular areas of affected eyes and contralateral/control eyes.

	CM ( <i>n</i> = 11) (A)	Macular of affected eyes ( <i>n</i> = 11) (B)	Macular of contralateral eyes ( <i>n</i> = 11) (C)	<i>p</i> value		
				AB	AC	BC
Panel a						
Sex (male/female)	6/5	6/5	6/5	–	–	–
Age (years)	43.36 ± 8.61	43.36 ± 8.61	43.36 ± 8.61	–	–	–
Eye (right/left)	8/3	8/3	3/8	–	–	–
Total vascular density (%)	67.990 ± 34.899	131.333 ± 27.807	154.208 ± 5.599	0	0	0.006
Centre of the ring (%)	5.640 ± 4.969	7.141 ± 3.211	8.558 ± 1.765	0.402	0.072	0.262
Inner-ring vascular density (%)						
Temporal	5.840 ± 4.935	13.774 ± 4.315	16.333 ± 3.959	0.001	0	0.310
Superior	6.654 ± 4.811	14.799 ± 4.019	16.966 ± 4.170	0	0	0.292
Nasal	8.620 ± 5.438	14.833 ± 5.566	16.666 ± 4.126	0.016	0.001	0.623
Inferior	9.230 ± 5.939	13.499 ± 4.999	16.524 ± 4.012	0.082	0.003	0.304
Outer-ring vascular density (%)						
Temporal	6.480 ± 4.191	12.674 ± 3.655	14.983 ± 3.621	0.001	0	0.346
Superior	8.890 ± 5.063	14.483 ± 4.568	16.791 ± 4.170	0.013	0.001	0.421
Nasal	11.880 ± 5.746	16.499 ± 6.091	18.383 ± 4.592	0.085	0.008	0.636
Inferior	9.020 ± 5.605	13.766 ± 5.251	16.441 ± 4.160	0.056	0.002	0.391
Panel b						
Total perfusion density (%)	1.617 ± 0.847	3.152 ± 0.714	3.662 ± 0.127	0	0	0.01
Centre of the ring (%)	0.135 ± 0.116	0.476 ± 1.079	0.507 ± 1.067	0.334	0.288	0.322
Inner-ring perfusion density (%)						
Temporal	0.138 ± 0.118	0.634 ± 0.1030	0.697 ± 1.007	0.147	0.098	0.275
Superior	0.161 ± 0.119	0.671 ± 1.017	0.718	0.133	0.097	0.307
Nasal	0.206 ± 0.134	0.668 ± 1.022	0.707 ± 1.004	0.172	0.134	0.308
Inferior	0.218 ± 0.147	0.634 ± 1.032	0.709 ± 1.003	0.221	0.142	0.271
Outer-ring perfusion density (%)						
Temporal	0.155 ± 0.105	0.619 ± 1.034	0.677 ± 1.014	0.175	0.122	0.291
Superior	0.214 ± 0.123	0.679 ± 1.016	0.732 ± 0.996	0.167	0.120	0.289
Nasal	0.291 ± 0.144	0.724 ± 1.006	0.763 ± 0.986	0.194	0.151	0.300
Inferior	0.216 ± 0.138	0.653 ± 1.027	0.724 ± 0.999	0.199	0.128	0.268

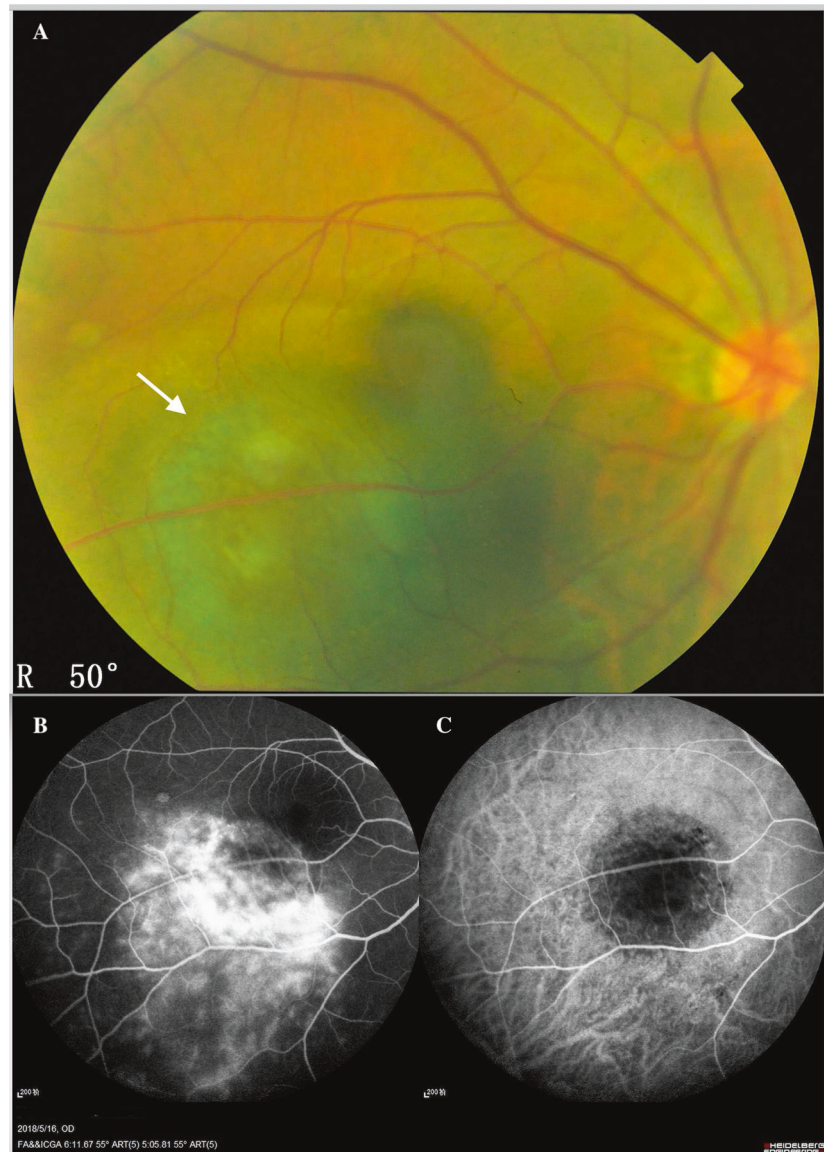
Data were presented as mean ± SD; statistical analyses were Student's *t* test.

OCT system provided by Carl Zeiss Meditec, Inc.), spectral domain, the OCT system operating at superluminescent diode 840-nm wavelength and 68-kHz axial scan repetition rate. Using the complex optical microangiography algorithm to generate the OCTA images and the additional scans by the 20-Hz fastTrac™ technology provides live tracking for motion-artefact-free images [12]. The AngioPlex Matrix™ technology provides the measure of VD and PD images. The Single-Scan Simplicity of the ZEISS AngioPlex requires only a single additional OCT scan to generate an ultra-clear three-dimensional (3D) OCTA image. 3D horizontal and vertical OCTA raster data were acquired in retina mode (6 × 6 mm, 8 × 8 mm) with scan depth of 2 mm in tissue. Each OCTA raster scan took about 2.5 s to acquire

three repeated B scans. The software automatically segmented the tissue into six layers: the vitreoretinal interface, the superficial retinal vascular layer (SRL), the deep retinal vascular layer, the avascular, the choriocapillaris and the choroid layer. For the SRL, the VD and PD were calculated separately in nine regions (central, inner superior, inner inferior, inner temporal, inner nasal, outer superior, outer inferior, outer temporal and outer nasal), and the total area. The congruency between both methods was evaluated. The CM surface and the boundary of the CM-pigmented epithelial layer were segmented in cross-sectional OCT images. For CM patients, editing each layer to avoid the errors for the thickness of the tumours may cause the algorithms to incorrectly trace the actual boundaries. Quantitative data

**Fig. 1 Inferior temporal choroidal melanoma of the left eye of a 45-year-old man. A**

Fundus colour photography showed that the CM was a brown mass (white arrow) located in the posterior fundus, which could not visualise the intrinsic blood vessels of the tumour. **B** The fluorescein angiographic (FA) showed the mottled hyperfluorescence in the early stage and the variable-increase hyperfluorescence with leakage in the late stage. The indocyanine green angiography (**C**) showed the minor hyperfluorescence in the early stage, which could not reveal the appearance of the CM vasculature.



were achieved within the entire VD of the image centred on the foveal avascular zone (FAZ), as previously described [13]. The VD and PD were measured automatically by the software in AngioPlex Metrix™ OCTA that quantified vessel density of a local region of tissue according to Early Treatment of Diabetic Retinopathy Study subfields [14]. The FAZ could not be perfectly delineated in some of the cases owing to its disappearance for the location of the tumour. Therefore, we decided not to include the FAZ as our main quantitative data.

### Statistical analysis

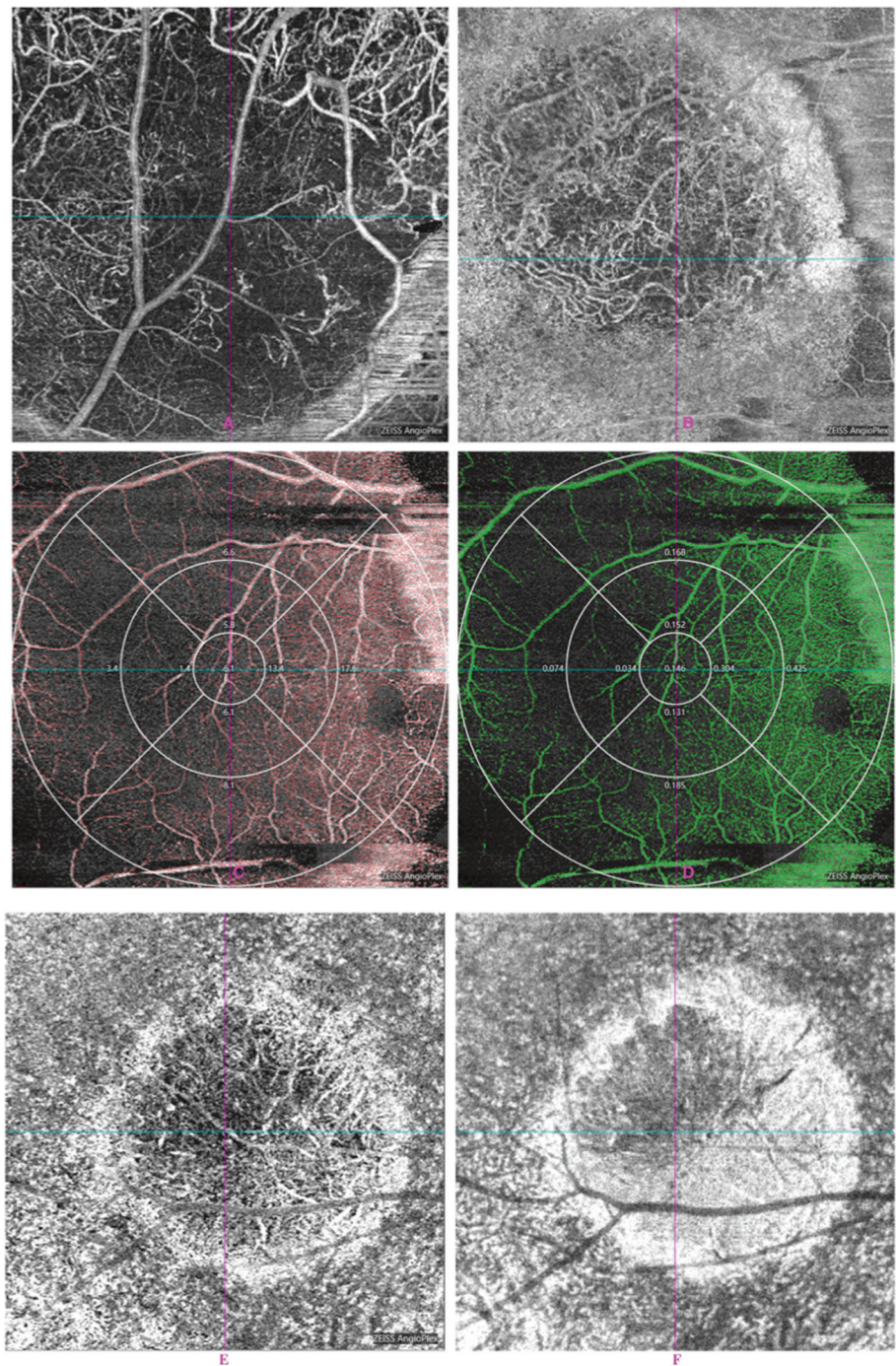
Student's *t* test was used to compare the VD and PD measurements between CM, macular area of the affected eyes and their contralateral eyes. Statistical analysis was

performed using a statistical software package (SPSS for Mac, version 22.0, IBM-SPSS, Chicago, IL). Measurements obtained before and after the DRPPT were compared with each other using the paired Student's *t* test. All measurements were described as mean  $\pm$  standard error. All *p* values were based on two-sided tests and considered statistically significant if  $<0.05$ .

### Results

Eyes each of 11 patients (6 males, 5 females; mean average age  $43.36 \pm 8.61$  years, range 33–55 years) with CM were prospectively included in this observational case series. The clinical diagnosis information of CM patients is listed in Table 2. Five of 11 patients who underwent the treatment

**Fig. 2 OCTA in patient eyes showed intratumoural vasculature of the CM. A, B** About 840-nm Retina Depth Encoded OCTA in patient eyes showed blood vessels in the CM with predominantly heterogeneously distributed and disorganised intratumoural vasculature. There was good penetration of flow signal in the CM in OCTA. The vascular and perfusion density within CM were measured from AngioPlex Metrix™ OCTA images. **C, D** The vascular and perfusion density in CM and macular areas were measured from AngioPlex Metrix™ OCTA images. Nine main regions were evaluated for the purposes of this study (6 × 6 mm). **C** Vascular density (VD), **D** perfusion density (PD). **E, F** After radiation treatment, OCTA that showed the progressive reduction in tumour vessel density over time was observed in choroidal melanomas treated with radioactive plaques. **E** Pre-PRT. **F** Aft-PRT.



with I-125 plaque brachytherapy were planned. In the post-treatment group, two patients were male and three were female, with a mean age of  $45.35 \pm 5.36$  years (range 33–51 years). Retina Depth Encoded OCTA in patient eyes clearly visualised blood vessels in the CM with predominantly heterogeneously distributed and disorganised intratumoural vasculature, which was inconsistent with the previously described FA/ICGA appearances of the CM vasculature (Fig. 1). There was good penetration of blood-flow signals

in the tumour lesions and macular areas in OCTA (6 × 6 mm). Furthermore, the dome-shaped elevation of melanomas and densely pigmented part of the tumour does not block the visualisation of the vessels by OCT signal.

OCTA performed better visualisation of CM than conventional fundus angiography (Fig. 2). OCTA of CM showed an increase in tumour vascularity associated with the lesions. In 11 eyes with CM, the OCTA showed heterogeneously distributed dense vasculature intrinsic to the

mass, tumour blood vessels are rich and ring-like and the small vascular loops were noted (Fig. 2A, B). The areas of attenuated signals may indicate the absence of vascularity or very densely packed cells.

The 840-nm OCT can show the full thickness (3 mm) of the pigmented tumour lesions. The 840-nm OCTA showed increased vascularity composed of many tortuous ring loops in the tumour (Fig. 2A, B). OCTAs demonstrated that the intratumoural blood vessels were extremely dense and disorganised. In addition, the tumour vasculature was not masked by the pigmentation of melanin deposition in the CM at 840-nm OCTA. In cases of moderate pigmented CMs, cross-sectional OCTA revealed that most of the blood vessels were located within the tumour. In cases of thick pigmented CMs, there was still very dense vasculature with disordered blood-vessel loops. The VD and PD within CM were measured from AngioPlex Metrix™ OCTA images.

The macular areas in the eyes of CM patients and their contralateral healthy eyes were evaluated with OCTA. The VD and PD within contralateral healthy eyes of CM patients were measured from AngioPlex Metrix™ OCTA images. Nine main regions were evaluated for the purpose of this study (Fig. 2C, D). The VD and PD in the tumour area ( $67.990 \pm 34.899\%$ ,  $1.617 \pm 0.847\%$ ,  $p < 0.0001$ ) were significantly lower when compared to the macular area of the affected eyes ( $131.333 \pm 27.807\%$ ,  $3.152 \pm 0.714\%$ ,  $p < 0.0001$ ) and the macular area of contralateral eyes ( $154.208 \pm 5.599\%$ ,  $3.662 \pm 0.127\%$ ,  $p < 0.0001$ ) (Table 1 and Fig. 3A–D), whose VD and PD are repeatable and reproducible using optical microangiography-based OCTA. There were no significant differences in the FAZ of macular-compared affected eyes with contralateral eyes (Fig. 4).

Five eyes with CM of five patients underwent the treatment of PRT. After radiation treatment, the VD and PD ( $116.526 \pm 7.598\%$ ,  $2.438 \pm 0.358\%$ ,  $p < 0.05$ ) were significantly lower than before treatment ( $141.544 \pm 14.645\%$ ,  $3.327 \pm 0.354\%$ ,  $p < 0.05$ ) (Figs. 2E, F and 3E, F). A progressive decrease in tumour VD over time was observed in CM treated with I-125 plaque brachytherapy.

In our study, 840-nm OCTA could see the full thickness in the range of 1.3–4.8 mm; however, it could not completely penetrate the thicker CMs (the thickness measured by ultrasonography is 5.37 and 6.46 mm, respectively). The 840-nm OCTA provided good penetration to show high VD on AngioPlex Metrix™ angiography in most tumours, even in a few cases of highly pigmented CM. It could be seen that dense pigmentation at the CM did not block the display of tumour blood vessels; the tumour vessels could be seen in the pigmented part of the tumour, and demonstrated tortuous blood vessels, uneven thickness and relatively disorganised intratumoural vasculature.

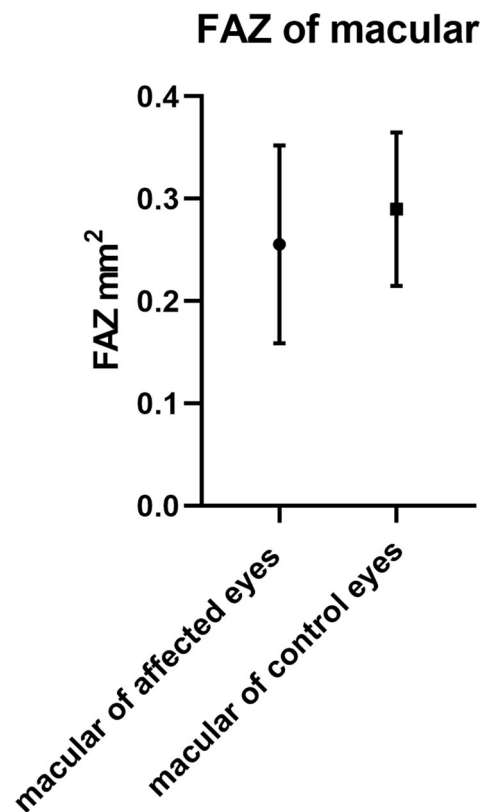


**Fig. 3** The FAZ in the eyes of CM patients and their contralateral healthy eyes were evaluated with OCTA. There were no significant differences in the FAZ of macular-compared affected eyes with contralateral/control eyes ( $0.255 \pm 0.096 \text{ mm}^2$ ,  $0.290 \pm 0.075 \text{ mm}^2$ ,  $p = 0.411 > 0.05$ ).

## Discussion

OCTA provides a unique, safe and fast technique for the evaluation of blood flow, VD and tissue perfusion, which has been applied to tumour-related research fields [15]. The imaging research of intraocular tumours with OCTA is a developing field; Chen et al. [16] used OCTA to visualise abundant vasculature within conjunctival racemose haemangioma not seen on FA. In this study, we prove that OCTA operating at 840 nm can be used to image CM and quantify intratumoural vascular and PD.

The growth of tumour is closely related to intratumoural vessels. Solid tumours experience the initial avascular and the subsequent vascular growth stage. Increased vascularity is a sign of malignant transformation [16, 17]. This happens through the process of angiogenesis in which neovascularization forms a network of disordered and highly permeable vascular network [18, 19], including the vasculogenic mimicry. Previous studies have confirmed that the increase of microvessel density in the tumour is related to the various measures of increased tumour invasiveness, which is a morphologic indicator of angiogenesis [20]. OCTA imaging does not depend on endothelial vascular channels, so it has the

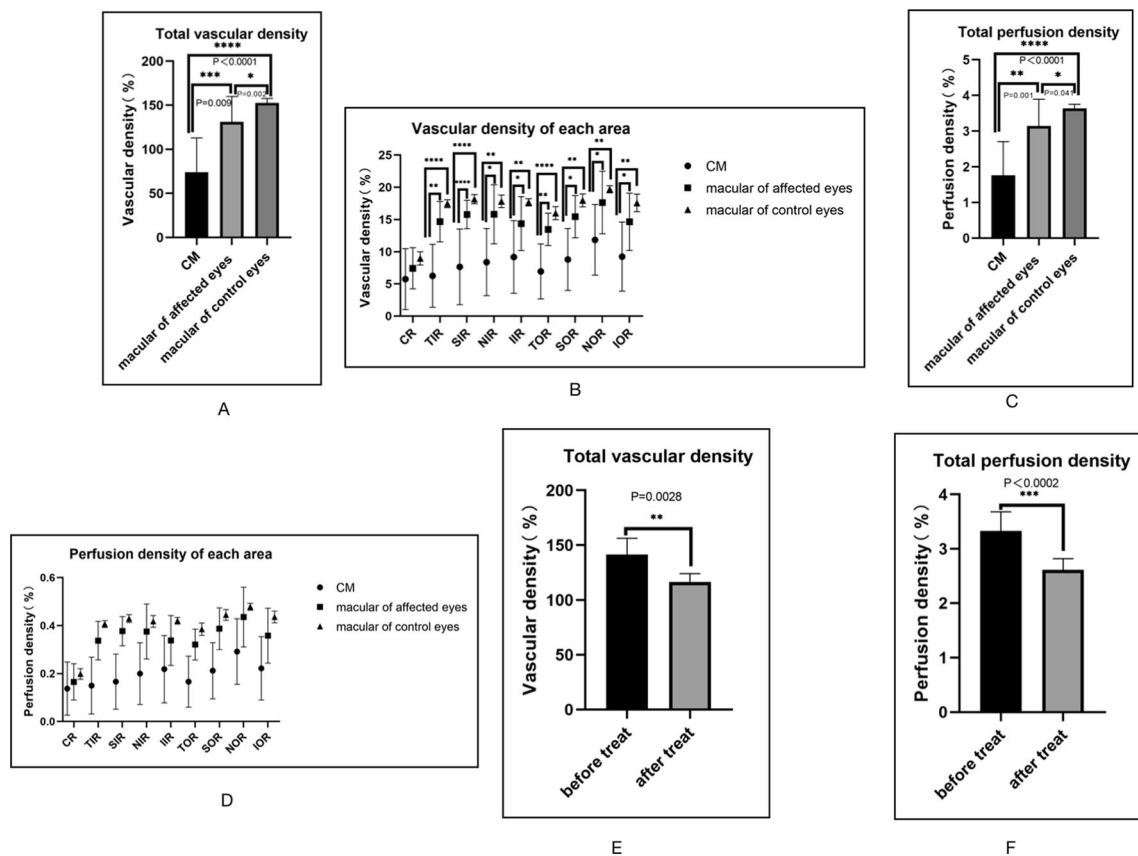


**Fig. 4** The vascular density and perfusion density in the eyes of CM patients and their contralateral healthy eyes were evaluated with OCTA. **A, B** Vascular-density comparisons in CM and macular areas of affected eyes and contralateral/control eyes. **A** Vascular-density comparison of the total areas. **B** Comparison of vascular density between CM and macular areas of affected eyes and contralateral/control eyes in nine areas. \*Compared with previous stage,  $p < 0.05$ . CR centre of the ring, IR inner ring, OR outer ring. **C, D** Perfusion-density comparisons in CM and macular areas of affected

eyes and contralateral/control eyes. **C** Perfusion-density comparison of the total areas. **D** Comparison of perfusion density between CM and macular of affected eyes and contralateral/control eyes in nine areas. \*Compared with previous stage,  $p < 0.05$ . CR centre of the ring, IR inner ring, OR outer ring. **E, F** The vascular and perfusion density of CM was significantly lower after treatment ( $116.526 \pm 7.598\%$ ,  $2.438 \pm 0.358\%$ ,  $p < 0.05$ ) than before treatment ( $141.544 \pm 14.645\%$ ,  $3.327 \pm 0.354\%$ ,  $p < 0.05$ ). **E** Vascular-density comparison. **F** Perfusion-density comparison.

potential to provide a non-invasive method for detection and quantification of microvessel density in tumours, and OCT of CM generally described a domed-shaped, smooth-surface topography with relatively fresh subretinal fluid demonstrating bushy photoreceptors [21], the mass with hyper-reflectivity at its anterior surface and dense posterior shadowing with an optically empty appearance. OCT does not reveal the internal properties of the tumour due to dense shadowing [22, 23].

However, OCTA could construct a map of blood flow and reveals the tumour vascularity, irrespective of the limitation of vascular endothelial structure and the pigmentation, as it utilised the movement of red blood cells against stationary tissues as intrinsic contrast, and the artefacts produced by the motion from patient movement are eliminated by post-imaging software. Detection of choroidal vascular flow rate in CM by OCTA has also been described previously; the OCTA imaging could differentiate choroidal

nevus from melanoma [24–27]. In this study, OCTA showed the presence of heterogeneously distributed small vessels and disorganised intratumoural vasculature within the tumour mass; CM is characterised by hyperplasia of blood vessels, which are disorganised and form tortuous loops in morphology and the increase in VD. Besides, we also proved that the tumour local control and the regression of lesions after radiotherapy are related to the reduction in the abnormal intratumoural vessel density. Previously, studies have investigated retinal vascular changes associated with radiotherapy for intraocular tumours [28–33]; however, tumour vascularity changes after I-125 plaque brachytherapy have not been described. The quantitative changes of VD and PD measured by OCTA may provide valuable information for tumour control or regression after radiotherapy.

In our study, eyes affected by CM as compared to the control group showed lower vascular and PD in the centre

of the measurement zone focused on macular areas ( $p < 0.0001$ ). These results agree with the findings obtained in previous studies, which also evaluated changes in retinal vasculature associated with intraocular tumours [29, 33, 34]. Interestingly, other single-measurement zones have no significant differences ( $p > 0.05$ ) in VD- and PD-compared CM with control eyes.

Patients with CM often have poor vision and the potential of life-threatening, but it is difficult to diagnose early small-melanoma lesions in morphology [24–27]. Excisional biopsy or radiotherapy for the treatment of CM can lead to considerable morbidity, and observation is related to the risk of tumour metastasis, which helps in finding a non-invasive method to help predict tumour behaviour that is necessary. Clinically, FA and ICGA have been previously considered as the conventional method to distinguish malignant tumours from benign lesions; however, FA/ICGA is invasive and has a risk associated with dye injections. In addition, the imaging of angiography was also obscured by variable pigmentation and haemorrhage, so this method could not fully visualise the blood vessels of tumour lesions and lacks the function of quantitation. OCTA could provide a non-invasive, convenient and safe alternative method for monitoring of choroidal tumours, and contributes to identifying those lesions with the highest risk of malignancy and metastasis. Using OCTA findings as a 'useful biomarker' for tumours that do not yet show other high-risk signs of metastasis, may make it easier for clinicians to detect concerning changes in intratumoural vasculature, and thus may also avoid unnecessary biopsy or radiotherapy.

Hence, OCTA might serve as a non-invasive tool to ascertain CM vascularity at different levels that might not be picked up on FA and OCT or both combined. However, a close follow-up is required to detect tumour growth or to confirm malignant transformation; OCTA findings can be used as an important marker to follow. Therefore, further research is necessary to determine the clinical application of this technique.

At present, there are several limitations of OCTA technology for imaging the intraocular tumours. First, the size of the OCTA scanning was limited and not enough to capture the entire retina. We studied both  $6 \times 6$ -mm and  $8 \times 8$ -mm scan sizes containing the same axial scan numbers, and we found that the  $6 \times 6$ -mm scan size was preferable as it provides better vascular details. Another important limitation of OCTA imaging of intraocular tumours is lack of penetration through heavily dense pigmented lesions and thicker tumours (with the best penetration seen to  $<4$  mm). Although not all CM can be imaged completely, the 840-nm OCTA system still has advantages in the penetration of tumours. In most tumours evaluated with the 840-nm system, both the AngioPlex

Metrix™ vascular pattern and the retinal pigment epithelium could be observed, which makes it possible to measure the VD and volume. Full OCTA penetration of the tumours appears to mainly depend upon the thickness of the tumour and its VD. The longer-wavelength systems may be able to overcome these defects, so as to successfully perform better OCTA imaging of intratumoural vascularity in tumours. OCTA technology cannot represent the impairment associated with the dysfunction of the inner vasculature, including leakage, bleeding or alteration of endothelial function.

## Conclusion

OCTA system can successfully image blood vessels in CM with variable pigmentation and  $<4$ -mm thickness. This technique can provide information concerning tumour microvasculature and has the advantages of quantitative measurement of vascular and PD within intraocular tumours, so it can be used as a reliable method to evaluate tumour vascularity and monitor the response to therapy.

## Summary

### What was known before

- Optical coherence tomography angiography (OCTA) is a relatively new, non-invasive and non-contact microvascular imaging technique.
- It can image angiography by detecting changes in the OCT signal when flowing blood cells pass through the vascular cavity.
- OCTA was originally applied to evaluate retinal vascular diseases or choroidal neovascularization.
- Analyzation and evaluation of tumour vasculature in humans by OCTA is a newly developing field.

### What this study adds

- Using OCTA, reliable detection and quantification of tumour vasculature is of high importance to study disease mechanisms and the effects of therapeutic approaches in the choroidal melanoma.

## Data availability

The data of this case report are available from the corresponding author on reasonable request.

## Acknowledgements

**Funding** The National Natural Science Foundation of China (Nr. 81272981), and the Beijing Natural Science Foundation (Nr. 7151003) provided financial support. Funding support was used to reimburse the travel-related expenses of conference attendees (recipient: WW).

**Author contributions** WW: examination of the patient, interpretation of the results and writing the paper; ZN: interpretation of the results and writing/reviewing of the paper; XX: interpretation of the results and writing/reviewing of the paper. All authors read and approved the final paper.

## Compliance with ethical standards

**Conflict of interest** The authors declare that they have no conflict of interest.

**Consent for publication** All authors consent to publish the paper.

**Ethical approval** The study followed the tenets of the Declaration of Helsinki and its ethical standards of 1964. The study was approved by the Medical Ethics Committee of the Beijing Tongren Hospital.

**Informed consent** Written informed consent was obtained from all participants.

**Publisher's note** Springer Nature remains neutral with regard to jurisdictional claims in published maps and institutional affiliations.

## References

- Jia Y, Bailey ST, Wilson DJ, Tan OU, Klein ML, Flaxel CJ, et al. Quantitative optical coherence tomography angiography of choroidal neovascularization in age-related macular degeneration. *Ophthalmology*. 2014;121:1435–44.
- Jia Y, Bailey ST, Hwang TS, McClintic SM, Gao SS, Pennesi ME, et al. Quantitative optical coherence tomography angiography of vascular abnormalities in the living human eye. *Proc Natl Acad Sci USA*. 2015;112:E2395–402.
- Cennamo G. OCT angiography examination of choroidal nevi and melanomas. In: Lumbroso B., Huang D., Jia, Y., et al., editors. *Clinical OCT angiography atlas*. New Delhi: Jaypee Brothers Medical Publishers, Ltd; 2015. p. 150–5.
- Ang M, Cai Y, Shahipasand S, Sim DA, Keane PA, Sng CCA, et al. En face optical coherence tomography angiography for corneal neovascularisation. *Br J Ophthalmol*. 2016;100:616–21.
- Wilkes SR, Robertson DM, Kurland LT, Campbell RJ. Incidence of uveal malignant melanoma in the resident population of Rochester and Olmsted County, Minnesota. *Am J Ophthalmol*. 1979;87:639–41.
- Singh AD, Turell ME, Topham AK. Uveal melanoma: trends in incidence, treatment, and survival. *Ophthalmology*. 2011;118:1881–5.
- Mahendraraj K, Lau C, Lee I, Chamberlain R. Trends in incidence, survival, and management of uveal melanoma: a population-based study of 7,516 patients from the Surveillance, Epidemiology, and End Results database (1973–2012). *Clin Ophthalmol*. 2016;10:2113–9.
- Desjardins L, Lumbroso L, Levy C, Mazal A, Delacroix S, Rosenwald JC, et al. Treatment of uveal melanoma with iodine 125 plaques or proton beam radiotherapy: indications and comparison of local recurrence rates. *J Fr Ophtalmol*. 2003;26:269–76.
- Damato B, Kacperek A, Chopra M, Campbell IR, Errington RD. Proton beam radiotherapy of choroidal melanoma: the Liverpool-Clatterbridge experience. *Int J Radiat Oncol Biol Phys*. 2005;62:1405–11.
- Dendale R, Rouic LL-L, Noel G, Feuvret L, Levy C, Delacroix S, et al. Proton beam radiotherapy for uveal melanoma: results of Curie Institut-Orsay proton therapy center (ICPO). *Int J Radiat Oncol Biol Phys*. 2006;65:780–7.
- Marconi DG, Castro DG, Rebouças LM, Gil GOB, Fogaroli RC, Maia MAC, et al. Tumor control, eye preservation, and visual outcomes of ruthenium plaque brachytherapy for choroidal melanoma. *Brachytherapy*. 2013;12:235–9.
- Spaide RF, Fujimoto JG, Waheed NK. Image artifacts in optical tomography angiography. *Retina*. 2015;35:2163–80. <https://doi.org/10.1097/IAE.0000000000000765>.
- Lupidi M, Coscas F, Cagini C, Fiore T, Spaccini E, Fruttini D, et al. Automated quantitative analysis of retinal microvasculature in normal eyes on optical coherence tomography angiography. *Am J Ophthalmol*. 2016;169:9–23.
- Lei J, Durbin MK, Shi Y, Uji A, Balasubramanian S, Baghdasaryan E, et al. Repeatability and reproducibility of superficial macular retinal vessel density measurements using optical coherence tomography angiography en face images. *JAMA Ophthalmol*. 2017;135:1092–8. <https://doi.org/10.1001/jamaophthalmol.2017.3431>.
- Vakoc BJ, Fukumura D, Jain RK, Bouma BE. Cancer imaging by optical coherence tomography: preclinical progress and clinical potential. *Nat Rev Cancer*. 2012;12:363–8.
- Chien JL, Sioufi K, Shields CL. Optical coherence tomography angiography of conjunctival racemose hemangioma. *Ophthalmology*. 2017;124:449.
- Folkman J. Tumor angiogenesis: therapeutic implications. *N Engl J Med*. 1971;285:1182–6.
- Ribatti D. Judah Folkman, a pioneer in the study of angiogenesis. *Angiogenesis*. 2008;11:3–10.
- Nishida N, Yano H, Nishida T, Kamura T, Kojiro M. Angiogenesis in cancer. *Vasc Health Risk Manag*. 2006;2:213–9.
- Weidner N. Intratumor microvessel density as a prognostic factor in cancer. *Am J Pathol*. 1995;147:9–19.
- Shields CL, Kaliki S, Rojanaporn D, Ferenczy SR, Shields JA. Enhanced depth imaging optical coherence tomography of small choroidal melanoma: comparison with choroidal nevus. *Arch Ophthalmol*. 2012;130:850–6.
- Cennamo G, Romano MR, Breve MA, Velotti N, Reibaldi M, de Crecchio G, et al. Evaluation of choroidal tumors with optical coherence tomography: enhanced depth imaging and OCT-angiography features. *Eye*. 2017;31:906–15. <https://doi.org/10.1038/eye.2017.14>.
- Shields CL, Manalac J, Das C, Ferguson K, Shields JA. Choroidal melanoma: clinical features, classification, and top 10 pseudo-melanomas. *Curr Opin Ophthalmol*. 2014;25:177–85.
- Ghassemi F, Mirshahi R, Fadakar K, Sabour S. Optical coherence tomography angiography in choroidal melanoma and nevus. *Clin Ophthalmol*. 2018;12:207–14. <https://doi.org/10.2147/OPHT.S148897>.
- Ghassemi F, Mirshahi R, Fadakar K, Sabour S. Optical coherence tomography angiography in choroidal melanoma and nevus. *Clin Ophthalmol*. 2018;22:207–14. <https://doi.org/10.2147/OPHT.S148897>.
- Toledo JJ, Asencio M, García JR, Morales LA, Tomkinson C, Cajjal C. OCT angiography: imaging of choroidal and retinal tumors. *Ophthalmol Retina*. 2018;2:613–22. <https://doi.org/10.1016/j.oret.2017.10.006>.

27. Valverde-Megías A, Say EAT, Ferenczy SR, Shields CL. Differential macular features on optical coherence tomography angiography in eyes with choroidal nevus and melanoma. *Retina*. 2017;37:731–40. <https://doi.org/10.1097/IAE.0000000000001233>.
28. Eldaly H, Eldaly Z. Melanocytoma of the optic nerve head, thirty-month follow-up. *Semin Ophthalmol*. 2015;30:464–9. <https://doi.org/10.3109/08820538.2013.874485>.
29. Veverka KK, AbouChehade JE, Iezzi R Jr, Pulido JS. Non-invasive grading of radiation retinopathy: the use of optical coherence tomography angiography. *Retina*. 2015;35:2400–10.
30. Matet A, Daruich A, Zografos L. Radiation maculopathy after proton beam therapy for uveal melanoma: optical coherence tomography angiography alterations influencing visual acuity. *Invest Ophthalmol Vis Sci*. 2017;58:3851–61.
31. Skalet AH, Liu L, Binder C, Miller AK, Wang J, Wilson DJ, et al. Quantitative OCT angiography evaluation of peripapillary retinal circulation after plaque brachytherapy. *Ophthalmol Retina*. 2018;2:244–50. <https://doi.org/10.1016/j.oret.2017.06.005>.
32. Skalet AH, Liu L, Binder C, Miller AK, Crilly R, Hung AY, et al. Longitudinal detection of radiation-induced peripapillary and macular retinal capillary ischemia using OCT angiography. *Ophthalmol Retina*. 2020;4:320–6. <https://doi.org/10.1016/j.oret.2019.10.001>.
33. Shields CL, Say EA, Samara WA, Khoo CT, Mashayekhi A, Shields JA. Optical coherence tomography angiography of the macula after plaque radiotherapy of choroidal melanoma: comparison of irradiated versus nonirradiated eyes in 65 patients. *Retina*. 2016;36:1493–505.
34. Skalet AH, Li Y, Lu CD, Jia Y, Lee BK, Husvogt L, et al. Optical coherence tomography angiography characteristics of iris melanocytic tumors. *Ophthalmology*. 2017;124:197–204. <https://doi.org/10.1016/j.optha.2016.10.003>.